ChemComm

Check for updates

Magnetic interactions in the $S = 1/2$ square-lattice antiferromagnets Ba_2CuTeO_6 and Ba_2CuWO_6: parent phases of a possible spin liquid†

Otto Mustonen, [*ab] Sami Vasala, [cd] Heather Mutch, [b] Chris I. Thomas, [a] Gavin B. G. Stenning, [e] Elisa Baggio-Saitovitch, [c] Edmund J. Cussen [b] and Maarit Karppinen [*a]

The isostructural double perovskites Ba_2CuTeO_6 and Ba_2CuWO_6 are shown by theory and experiment to be frustrated square-lattice antiferromagnets with opposing dominant magnetic interactions. This is driven by differences in orbital hybridisation of Te^{6+} and W^{6+}. A spin-liquid-like ground state is predicted for $Ba_2Cu(Te_{1-x}W_x)O_6$ solid solution similar to recent observations in $Sr_2Cu(Te_{1-x}W_x)O_6$.

Magnetic frustration can stabilise novel quantum ground states such as quantum spin liquids or valence bond solids.[1] Frustration occurs when not all of the magnetic interactions in a material can be satisfied simultaneously as a result of lattice geometry or competing interactions. We have recently shown that a quantum-spin-liquid-like state forms in the double perovskite solid solution $Sr_2Cu(Te_{1-x}W_x)O_6$ with a square lattice of Cu^{2+} ($3d^9$, $S = 1/2$) cations.[2,3] This was the first observation of a spin-liquid-like state in a square-lattice compound after 30 years of theoretical predictions.[4–8]

The parent compounds Sr_2CuTeO_6 and Sr_2CuWO_6 are frustrated square-lattice (FSL) antiferromagnets.[9–13] The FSL model (Fig. 1) has two interactions: nearest-neighbour J_1 interaction (side) and next-nearest-neighbour J_2 interaction (diagonal). Dominant antiferromagnetic J_1 leads to Néel type antiferromagnetic order and dominant J_2 leads to columnar magnetic order. Magnetic frustration arises from the competition of J_1 and J_2, and a quantum spin liquid state has been predicted for $J_2/J_1 = 0.5$ where frustration is maximised.[4–8]

[a] *Department of Chemistry and Materials Science, Aalto University, FI-00076 Espoo, Finland. E-mail: maarit.karppinen@aalto.fi, ohj.mustonen@gmail.com*

[b] *Department of Materials Science and Engineering, University of Sheffield, Mappin Street, Sheffield S1 3JD, UK*

[c] *Centro Brasileiro de Pesquisas Físicas (CBPF), Rua Dr Xavier Sigaud 150, Urca, Rio de Janeiro, 22290-180, Brazil*

[d] *Technische Universität Darmstadt, Institut für Materialwissenschaft, Fachgebiet Materialdesign durch Synthese, Alarich-Weiss-Straße 2, 64287 Darmstadt, Germany*

[e] *ISIS Neutron and Muon Source, Rutherford Appleton Laboratory, Harwell Science and Innovation Campus, Didcot, OX11 0QX, UK*

† Electronic supplementary information (ESI) available: Supporting computational and experimental details, figures and tables. See DOI: 10.1039/c8cc09479a

Sr_2CuTeO_6 and Sr_2CuWO_6 are the first known isostructural FSL systems with different dominant interactions and magnetic structures: dominant J_1 and Néel order for Sr_2CuTeO_6 and dominant J_2 and columnar order for Sr_2CuWO_6 respectively.[9,10] The two compounds have a tetragonal $I4/m$ double perovskite structure with nearly identical bond distances and angles.[11,13] The magnetism becomes highly two-dimensional as a result of a Jahn–Teller distortion as the only unoccupied Cu orbital $3d_{x^2-y^2}$ is in the ab square plane. The major differences in dominant magnetic interactions are due to the diamagnetic Te^{6+} d^{10} and W^{6+} d^0 cations located in the middle of the Cu^{2+} square (Fig. 1c), which hybridise differently with O 2p allowing different super-exchange paths between the Cu^{2+} cations.[14,15] The spin-liquid-like ground state forms when these two perovskites are mixed into a $Sr_2Cu(Te_{1-x}W_x)O_6$ solid solution.[2,3,16] Muon spin relaxation
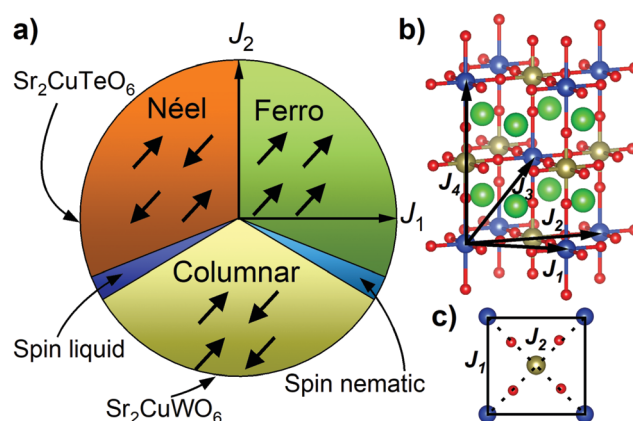

Fig. 1 (a) Phase diagram of the frustrated square-lattice model. Antiferromagnetic (negative) J_1 stabilises Néel order and J_2 columnar order respectively. A spin liquid state has been predicted for the Néel–columnar boundary at $J_2/J_1 = 0.5$ where magnetic frustration is maximised. (b) The double perovskite structure of $(Ba,Sr)_2Cu(Te,W)O_6$. J_1 and J_2 are the in-plane interactions of the FSL model, whereas J_3 and J_4 are out-of-plane interactions. The blue, dark yellow, red and green spheres represent Cu, Te/W, O and Ba/Sr, respectively. (c) The Cu^{2+} square in the ab plane with J_1 and J_2 interactions.

experiments revealed the absence of magnetic order or static magnetism in a wide composition range of $x = 0.1$–0.6.[2,3] The specific heat displays T-linear behaviour suggesting gapless excitations in a similar composition range.[2,3,16] The ground state has been proposed to be a random-singlet state with a disordered arrangement of non-magnetic valence bond singlets.[17,18]

Motivated by these exciting findings in the $Sr_2Cu(Te_{1-x}W_x)O_6$ system, we have investigated the magnetic interactions of the isostructural barium analogues Ba_2CuTeO_6 and Ba_2CuWO_6. Ba_2CuWO_6 is known to have columnar magnetic order,[19,20] but little is known about Ba_2CuTeO_6 as the perovskite phase requires high pressures to synthesise.[21] Here we use density functional theory (DFT) calculations and high-temperature series expansion (HTSE) fitting of experimental susceptibility data to show that these compounds are FSL antiferromagnets with opposite dominant interactions similar to Sr_2CuTeO_6 and Sr_2CuWO_6. We predict a quantum-spin-liquid-like state in $Ba_2Cu(Te_{1-x}W_x)O_6$ with strong antiferromagnetic interactions.

Magnetic interactions and electronic structure in Ba_2CuTeO_6 and Ba_2CuWO_6 were calculated using the DFT+U framework, where an on-site Coulomb repulsion term U was used to model electron correlation effects of localised Cu 3d orbitals. Interactions up to the fourth-nearest neighbour were evaluated, see Fig. 1b. J_1 and J_2 are the square plane interactions of the FSL model, and J_3 and J_4 are additional out-of-plane interactions. Energies of different spin configurations were mapped onto a Heisenberg Hamiltonian to obtain J_1–J_4. We have previously shown this approach works well for Sr_2CuWO_6.[10] The J_1 and J_2 interactions were also determined from experimental magnetic susceptibility data using high-temperature series expansion fitting. Ba_2CuTeO_6 was prepared by high-pressure synthesis and Ba_2CuWO_6 by conventional solid state synthesis. Details of the DFT calculations, sample synthesis and characterisation are available in the ESI.†

The calculated magnetic interactions of Ba_2CuTeO_6 and Ba_2CuWO_6 are presented in Table 1. The calculated values depend on the Coulomb U term as is typical with DFT+U, but the same

trends are observed for reasonable values of U. Despite being isostructural, the magnetic interactions in Ba_2CuTeO_6 and Ba_2CuWO_6 are very different. Ba_2CuTeO_6 has a very dominant antiferromagnetic J_1 interaction with weak J_2, J_3 and J_4 interactions. It is a near-ideal FSL Néel antiferromagnet. Ba_2CuWO_6, in contrast, has a dominant antiferromagnetic J_2 interaction slightly frustrated by an antiferromagnetic J_1 interaction with negligible J_3 and J_4 interactions. The strong J_2 interaction is consistent with the known columnar magnetic structure of this compound.[20] Due to the weakness of the out-of-plane J_3 and J_4 interactions, magnetism in both compounds is highly two-dimensional and well described by the FSL model.

The significant differences in the magnetic interactions of Ba_2CuTeO_6 and Ba_2CuWO_6 can be explained by their electronic structures. We have plotted total and partial densities of states for both compounds in Fig. 2. Ba_2CuTeO_6 and Ba_2CuWO_6 are antiferromagnetic insulators: the band gaps open between the occupied Cu 3d states hybridised with O 2p (valence band) and the unoccupied Cu $3d_{x^2-y^2}$ states hybridised with O 2p (conduction band). In Ba_2CuWO_6 the conduction band is further hybridised
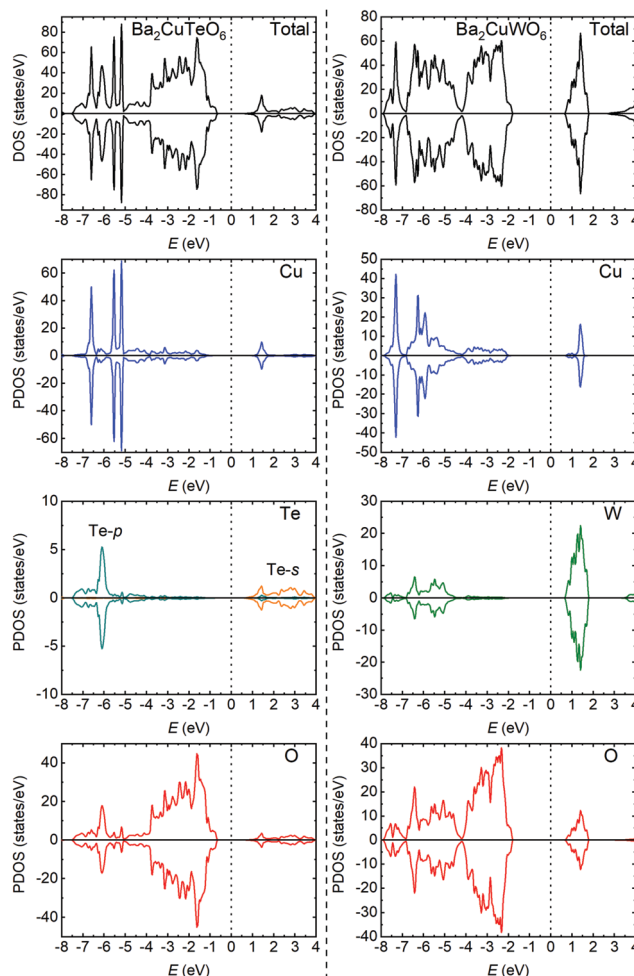

Fig. 2 Total and partial density of states plots for Ba_2CuTeO_6 (left) and Ba_2CuWO_6 (right). Both compounds are antiferromagnetic insulators. The moderate Te 5p/5s−O 2p hybridisation and stronger W 5d−O 2p hybridisation are seen in the Te/W and O PDOS plots.

Table 1 Exchange constants of Ba_2CuTeO_6 and Ba_2CuWO_6 obtained by density functional theory using different on-site Coulomb U terms and by high-temperature series expansion fitting of magnetic susceptibility data. Negative (positive) values correspond to antiferromagnetic (ferromagnetic) interactions

	$U = 7$ eV	$U = 8$ eV	$U = 9$ eV	HTSE
Ba_2CuTeO_6				
J_1 (meV)	−23.65	−20.22	−17.22	−16.54(3)
J_2 (meV)	0.13	0.23	0.06	−0.04(3)
J_3 (meV)	1.28	0.83	0.67	—
J_4 (meV)	−0.30	0.01	0.05	—
J_2/J_1	−0.01	−0.01	−0.003	0.002
Ba_2CuWO_6				
J_1 (meV)	−1.25	−1.17	−1.27	0.2(9)
J_2 (meV)	−14.71	−11.94	−9.56	−10.0(1)
J_3 (meV)	0.05	−0.01	0.01	—
J_4 (meV)	0.03	0.37	0.02	—
J_2/J_1	11.79	10.18	7.55	−50[a]

[a] Significant uncertainty in this value due to error in J_1.

with unoccupied W 5d states. The W 5d states also hybridise with the Cu 3d/O 2p states in the valence band, which allows a $180°$ Cu–O–W–O–Cu superexchange pathway resulting in a strong antiferromagnetic J_2 interaction. This hybridisation does not occur in Ba_2CuTeO_6 and therefore J_2 is negligible. In Ba_2CuTeO_6 the Te 5p states hybridise to a lesser degree with the Cu 3d/O 2p states in the conduction band, which could explain the strong antiferromagnetic J_1 interaction. However, the role of Te in the J_1 superexchange in Sr_2CuTeO_6 is under debate.[9,14] Overall, the electronic structures of Ba_2CuTeO_6 and Ba_2CuWO_6 are similar to their strontium analogues Sr_2CuTeO_6 and Sr_2CuWO_6, and the differences in magnetic interactions are driven by the same orbital hybridisation mechanism.

The experimental magnetic susceptibilities of synthesised Ba_2CuTeO_6 and Ba_2CuWO_6 samples are shown in Fig. 3. The broad maximum observed in the susceptibility is due to the two-dimensional nature of the magnetism in these materials. Our maximum temperature of 400 K was not enough for reliable Curie–Weiss fits. Previous measurements[21] up to 800 K yielded the Curie–Weiss constants $\Theta_{CW} = -400$ K for Ba_2CuTeO_6 and $\Theta_{CW} = -249$ K for Ba_2CuWO_6 revealing strong antiferromagnetic interactions.

The magnetic susceptibilities were fitted to a high-temperature series expansion of the FSL model.[22] The molar magnetic susceptibility χ_{mol} is given by:

$$\chi_{mol} = \frac{N_A g^2 \mu_B^2}{k_B T} \sum_n \beta^n \sum_m c_{m,n} x^m + \chi_0$$

where g is the effective g-factor, $\beta = -J_1/k_B$, $x = J_2/J_1$, χ_0 is a temperature independent diamagnetic correction and the coefficients $c_{m,n}$ are from Table 1 in ref. 22. The model has four parameters: J_1, J_2, g and χ_0, which were fitted to the experimental data using a least squares method. The model always produces two solutions due to internal symmetry: one with dominant J_1 and one with dominant J_2.[23] Our DFT calculations allow us to select the correct dominant J_1 solution for Ba_2CuTeO_6 and the dominant J_2 solution for Ba_2CuWO_6.

The best fits were obtained with the parameters $J_1 = -16.54(3)$ meV, $J_2 = -0.04(3)$ meV, $g = 2.20(1)$ for Ba_2CuTeO_6 and $J_1 = 0.2(9)$ meV, $J_2 = -10.0(1)$ meV, $g = 2.26(5)$ for Ba_2CuWO_6 in the temperature ranges 150–400 K and 90–400 K, respectively. The fitted exchange constants depend slightly on the minimum temperature used. For both compounds the calculated dominant interaction remains stable in a wide fitting range, but the weaker interaction cannot be accurately quantified. In Ba_2CuTeO_6 the sign of J_2 changes depending on the fitting range, whereas in Ba_2CuWO_6 the error of J_1 is much larger than its value. We can conclude, however, that the dominant interaction is much stronger than the weak one in both Ba_2CuTeO_6 ($|J_2|/|J_1| < 0.02$) and Ba_2CuWO_6 ($|J_1|/|J_2| < 0.12$) and that the DFT and HTSE results are in good agreement.

The magnetic properties of Ba_2CuTeO_6, Ba_2CuWO_6, Sr_2CuTeO_6 and Sr_2CuWO_6 are summarised in Table 2. Magnetic interactions in Ba_2CuTeO_6 and Ba_2CuWO_6 are notably stronger than their strontium analogues. This is due to the smaller $a^0a^0c^-$ tilt of the CuO_6 octahedra in the barium phases, which leads to stronger orbital overlap in the ab plane as the Cu–O–Te/W angle is closer to $180°$,[21] see ESI† for further details. As long-range magnetic order is driven by the weak out-of-plane interactions which are of the same order in all compounds, Ba_2CuTeO_6 and Ba_2CuWO_6 are even closer to ideal two-dimensional antiferromagnets than their strontium analogues. The transition temperature of Ba_2CuTeO_6 is not known, but we predict it to have the highest frustration index $f = \Theta_{CW}/T_N$ of these compounds and the Néel magnetic structure due to the very strong J_1 interaction. Magnetic excitations in Sr_2CuTeO_6 and Sr_2CuWO_6 have been observed at temperatures higher than $2T_N$ driven by the two-dimensional magnetic interactions.[9,10] The stronger in-plane J_1 and J_2 interactions of the barium phases indicate the excitations survive to even higher temperatures.

Since Ba_2CuTeO_6 has a dominant J_1 interaction and Ba_2CuWO_6 has a dominant J_2 interaction, we predict a spin-liquid-like state will form in the $Ba_2Cu(Te_{1-x}W_x)O_6$ solid solution similar to $Sr_2Cu(Te_{1-x}W_x)O_6$. In the $Sr_2Cu(Te_{1-x}W_x)O_6$ system the Néel order is destabilised already at $x = 0.1$, and spin-liquid-like state exist in the composition region $x = 0.1–0.6$. Columnar order is observed for $x = 0.7–1$. Since the J_1 interaction of Ba_2CuTeO_6 is so strong even compared to J_2 in Ba_2CuWO_6, we predict the Néel order remains more stable against W substitution. For the same reason, the columnar order near $x = 1$ is likely to be less stable in $Ba_2Cu(Te_{1-x}W_x)O_6$. The extent of the spin-liquid-like region depends also on disorder, and is difficult to predict just from the properties of the end phases. Finally, the stronger antiferromagnetic interactions in the barium phases indicate that the quantum disordered ground state will remain stable up to higher temperatures.

The previous discussion concerns a double perovskite $Ba_2Cu(Te_{1-x}W_x)O_6$ solid solution, which near $x = 0$ will require high-pressure synthesis to form. The ambient pressure form of Ba_2CuTeO_6 is triclinic with a tolerance factor higher than 1.03.[24] Therefore, a $Ba_2Cu(Te_{1-x}W_x)O_6$ solid solution prepared in
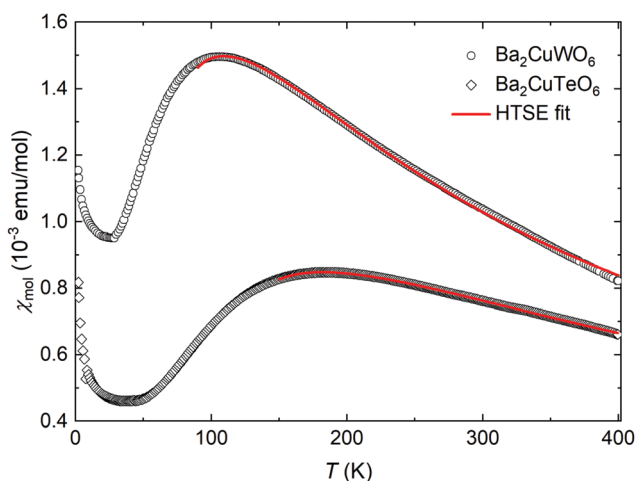

Fig. 3 Magnetic susceptibility and high-temperature series expansion fits for Ba_2CuTeO_6 and Ba_2CuWO_6. Open symbols represent experimental data and the lines are HTSE fits with the parameters $J_1 = -16.54(3)$ meV, $J_2 = -0.04(3)$ meV, $g = 2.20(1)$ and $J_1 = 0.2(9)$ meV, $J_2 = -10.0(1)$ meV, $g = 2.26(5)$ for Ba_2CuTeO_6 and Ba_2CuWO_6, respectively. The ZFC and FC curves overlap and therefore only ZFC data is shown.

Table 2 Magnetic properties of Ba_2CuTeO_6, Sr_2CuTeO_6, Ba_2CuWO_6 and Sr_2CuWO_6. Exchange interactions J_1 and J_2 have been obtained by density functional theory (DFT; $U = 8$ eV), high-temperature series expansion fitting (HTSE) or by inelastic neutron scattering (INS). The data for Ba_2CuTeO_6 and Ba_2CuWO_6 are from this work unless specified otherwise

	Ba_2CuTeO_6	Sr_2CuTeO_6	Ba_2CuWO_6	Sr_2CuWO_6
J_1 (meV)	−20.22 (DFT)	−7.18 (INS)[9]	−1.17 (DFT)	−2.45 (DFT)[10]
	−16.54(3) (HTSE)		−0.2(9) (HTSE)	−1.2 (INS)[10]
J_2 (meV)	0.23 (DFT)	−0.21 (INS)[9]	−11.94 (DFT)	−8.83 (DFT)[10]
	−0.04(3) (HTSE)		−10.0(1) (HTSE)	−9.5 (INS)[10]
Θ_{CW} (K)	−400[21]	−80[2]	−249[21]	−165[2]
T_N (K)	—	29[11]	28[20]	24[13]
$f = \Theta_{CW}/T_N$	—	2.8	8.9	6.9
k	$[1/2\ 1/2\ k_z]^a$	$[1/2\ 1/2\ 0]$[11]	$[0\ 1/2\ 1/2]$[20]	$[0\ 1/2\ 1/2]$[12]
Magnetic order	Néel[a]	Néel	Columnar	Columnar

[a] Predicted based on magnetic interactions.

ambient pressure will have a triclinic to tetragonal structural change at some composition. Triclinic Ba_2CuTeO_6 is a spin ladder system close to a quantum critical point,[25] and we propose Te-for-W substitution could drive the system from magnetic order to a spin singlet state.

In conclusion, we have investigated the magnetic interactions of the tetragonal double perovskites Ba_2CuTeO_6 and Ba_2CuWO_6 by DFT calculations and by HTSE fitting. Both compounds are well described by the frustrated square-lattice model as out-of-plane interactions are very weak. In Ba_2CuTeO_6 the antiferromagnetic nearest-neighbor J_1 interaction dominates ($|J_2|/|J_1| < 0.02$), whereas in Ba_2CuWO_6 the antiferromagnetic next-nearest neighbor interaction J_2 dominates ($|J_1|/|J_2| < 0.12$). The $Ba_2Cu(Te,W)O_6$ system is the second known FSL system where isostructural compounds have opposite magnetic interactions. This is driven by differences in orbital hybridisation of Te 5p/5s and W 5d with O 2p. A spin-liquid-like ground state is predicted for the $Ba_2Cu(Te_{1−x}W_x)O_6$ solid solution similar to the recent findings in the $Sr_2Cu(Te_{1−x}W_x)O_6$ system.

Conflicts of interest

There are no conflicts to declare.

Notes and references

1 L. Balents, *Nature*, 2010, **464**, 199–208.
2 O. Mustonen, S. Vasala, E. Sadrollahi, K. P. Schmidt, C. Baines, H. C. Walker, I. Terasaki, F. J. Litterst, E. Baggio-Saitovitch and M. Karppinen, *Nat. Commun.*, 2018, **9**, 1085.
3 O. Mustonen, S. Vasala, K. P. Schmidt, E. Sadrollahi, H. C. Walker, I. Terasaki, F. J. Litterst, E. Baggio-Saitovitch and M. Karppinen, *Phys. Rev. B*, 2018, **98**, 064411.
4 P. W. Anderson, *Science*, 1987, **235**, 1196–1198.
5 F. Mezzacapo, *Phys. Rev. B: Condens. Matter Mater. Phys.*, 2012, **86**, 045115.
6 H.-C. Jiang, H. Yao and L. Balents, *Phys. Rev. B: Condens. Matter Mater. Phys.*, 2012, **86**, 024424.
7 W.-J. Hu, F. Becca, A. Parola and S. Sorella, *Phys. Rev. B: Condens. Matter Mater. Phys.*, 2013, **88**, 060402.
8 W.-Y. Liu, S. Dong, C. Wang, Y. Han, H. An, G.-C. Guo and L. He, *Phys. Rev. B*, 2018, **98**, 241109.
9 P. Babkevich, V. M. Katukuri, B. Fåk, S. Rols, T. Fennell, D. Pajić, H. Tanaka, T. Pardini, R. R. P. Singh, A. Mitrushchenkov, O. V. Yazyev and H. M. Rønnow, *Phys. Rev. Lett.*, 2016, **117**, 237203.
10 H. C. Walker, O. Mustonen, S. Vasala, D. J. Voneshen, M. D. Le, D. T. Adroja and M. Karppinen, *Phys. Rev. B*, 2016, **94**, 064411.
11 T. Koga, N. Kurita, M. Avdeev, S. Danilkin, T. J. Sato and H. Tanaka, *Phys. Rev. B*, 2016, **93**, 054426.
12 S. Vasala, M. Avdeev, S. Danilkin, O. Chmaissem and M. Karppinen, *J. Phys.: Condens. Matter*, 2014, **26**, 496001.
13 S. Vasala, H. Saadaoui, E. Morenzoni, O. Chmaissem, T. Chan, J. Chen, Y. Hsu, H. Yamauchi and M. Karppinen, *Phys. Rev. B: Condens. Matter Mater. Phys.*, 2014, **89**, 134419.
14 Y. Xu, S. Liu, N. Qu, Y. Cui, Q. Gao, R. Chen, J. Wang, F. Gao and X. Hao, *J. Phys.: Condens. Matter*, 2017, **29**, 105801.
15 M. Zhu, D. Do, C. R. Dela Cruz, Z. Dun, H. D. Zhou, S. D. Mahanti and X. Ke, *Phys. Rev. Lett.*, 2014, **113**, 076406.
16 M. Watanabe, N. Kurita, H. Tanaka, W. Ueno, K. Matsui and T. Goto, *Phys. Rev. B*, 2018, **98**, 054422.
17 K. Uematsu and H. Kawamura, *Phys. Rev. B*, 2018, **98**, 134427.
18 L. Liu, H. Shao, Y.-C. Lin, W. Guo and A. W. Sandvik, *Phys. Rev. X*, 2018, **8**, 041040.
19 Y. Todate, *J. Phys. Soc. Jpn.*, 2001, **70**, 337.
20 Y. Todate, W. Higemoto, K. Nishiyama and K. Hirota, *J. Phys. Chem. Solids*, 2007, **68**, 2107–2110.
21 D. Iwanaga, Y. Inaguma and M. Itoh, *J. Solid State Chem.*, 1999, **147**, 291–295.
22 H. Rosner, R. R. P. Singh, W. H. Zheng, J. Oitmaa and W. E. Pickett, *Phys. Rev. B: Condens. Matter Mater. Phys.*, 2003, **67**, 014416.
23 A. A. Tsirlin, R. Nath, A. M. Abakumov, Y. Furukawa, D. C. Johnston, M. Hemmida, H. A. Krug Von Nidda, A. Loidl, C. Geibel and H. Rosner, *Phys. Rev. B: Condens. Matter Mater. Phys.*, 2011, **84**, 014429.
24 G. N. Rao, R. Sankar, A. Singh, I. P. Muthuselvam, W. T. Chen, V. N. Singh, G.-Y. Guo and F. C. Chou, *Phys. Rev. B*, 2016, **93**, 104401.
25 D. Macdougal, A. S. Gibbs, T. Ying, S. Wessel, H. C. Walker, D. Voneshen, F. Mila, H. Takagi and R. Coldea, *Phys. Rev. B*, 2018, **98**, 174410.